Occupation of fine-structure states in electron capture and transport

Marek Seliger,[1,2,*] Carlos O. Reinhold,[3,4] Tatsuya Minami,[3,5] David R. Schultz,[3] Shuhei Yoshida,[2] Joachim Burgdörfer,[2,4] Emily Lamour,[6] Jean-Pierre Rozet,[6] and Dominique Vernhet[6]

[1]*Institute for Physics, Karl-Franzens-University Graz, A-8010 Graz, Austria, EU*

[2]*Institute for Theoretical Physics, Vienna University of Technology, A-1040 Vienna, Austria, EU*

[3]*Physics Division, Oak Ridge National Laboratory, Oak Ridge, Tennessee 37831-6372, USA*

[4]*Department of Physics and Astronomy, University of Tennessee, Knoxville, Tennessee 37996-1200, USA*

[5]*Department of Physics, Auburn University, Auburn, Alabama 36849, USA*

[6]*Institut des NanoSciences de Paris, CNRS UMR 75-88, Université Paris 6, 75015 Paris, France, EU*

(Received 6 December 2007; published 16 April 2008)

We study the population of the fine-structure states in excited-state manifolds of hydrogenic Ar^{17+} ions resulting from charge transfer in collisions of 13.6 MeV/amu Ar^{18+} ions with thin carbon foils or CH_4 and N_2 gases. Experimental information on excited states populations is determined by x-ray spectroscopy of individual fine-structure components of the Lyman series allowing for sensitive probes of relativistic effects during the primary charge transfer and the subsequent transport. We show that the ratio of the populations of the $2p_{1/2}$ and $2p_{3/2}$ states provides clear evidence for spin dependent relativistic effects at moderately relativistic speeds.

DOI: 10.1103/PhysRevA.77.042713 PACS number(s): 34.50.Fa, 34.10.+x, 34.70.+e, 34.80.Nz

I. INTRODUCTION

Calculation of electron capture in collisions of highly charged ions with atoms represents a significant challenge due to the dynamical two-center nature of the problem and the large number of possible final channels including the continuum. Relativistic collisions considerably increase the complexity since it is approximately equivalent to increasing the dimensionality of the problem. Identifying the borderline between relativistic and nonrelativistic dynamics provides a unique and fundamental testing ground for the development of a universal description applicable in both regimes.

Relativistic effects in charge transfer are well documented at very high collision velocities $v_p/c \sim 1$ where, for asymmetric partners (projectile charge $\gg$ target nuclear charge), it is dominated by radiative electron capture [1–5]. In this work we explore relativistic effects in relatively low-velocity ($v_p = 23$ a.u., $v_p/c = 0.17$) collisions of fully stripped Ar^{18+} ions with various targets. These effects are identified by analyzing the population of individual fine-structure levels of the excited states of Ar^{17+} produced by electron capture. Relativistic effects result, generically, from two different sources: (i) relativistic dynamics in a violent collision on a short, typically subattosecond, time scale as $v_p \lesssim c$ inducing spin flips by Lorentz transformed motional fields or mixing the large with the small component of the Dirac four component vector. (ii) Relativistic motion of the electron in its initial and final atomic orbit leads to modified eigenenergies, i.e., fine-structure and Lamb shift. These relativistic structure effects in highly charged ions $Z_p \gg 1$ are present on much longer time scales. In the present study of capture and transport of excited states in solids, we find evidence for the interplay between these two contributions.

This work is an extension of a recent publication [6] analyzing excited state formation in Ar^{18+} traversing carbon foils. The dynamics of such collision system is quite complex. After an electron capture event takes place, the ion undergoes a sequence of multiple collisions, radiative decay, and intrashell mixing due to the wake field induced by the moving ion. This complexity is associated with the presence of different time scales governing the relevant interactions: the binary atomic collision time τ_{AC} ($\lesssim 10^{-18}$ s at moderately relativistic speeds), the wake-field mixing time τ_W, the mean spacing in time between subsequent electron-ion and electron-electron collisions in the solid, t_C, leading to decoherence and damping, and the radiative relaxation time τ_R. Additional time scales of relevance in the present context are the spin-precession time, the characteristic time associated with the relativistic fine-structure (FS) splitting, $\Delta\varepsilon_{FS}, \tau_{FS} \approx (\Delta\varepsilon_{FS})^{-1}$, and the time scale associated with the Lamb-shift splitting $\tau_L \cong (\Delta\varepsilon_L)^{-1}$. We show in the following that the population of the fine-structure levels depends sensitively on these competing time scales. In addition, we show that in the limit of very thin foils, where only a single collisional process within time τ_{AC} can take place, a clear discrepancy between simulations and experiments remains unaccounted for. This discrepancy is also found for collisions in gases under single collision conditions. For details of our calculations and experiments we refer to [6–9]. Atomic units are used throughout unless otherwise stated.

II. POPULATION RATIO FOR FINE-STRUCTURE STATES

Consider the interaction of a 13.6 MeV/amu Ar^{18+} ion with a target T consisting of either a thin carbon foil or CH_4 and N_2 gases. Charge transfer in these collision systems is expected to be dominated by mechanical (i.e., nonradiative) electron capture from the lowest lying $1s$ electronic states of C or N. The interaction leads to a distribution of excited states

$$Ar^{18+} + T(1s) \rightarrow Ar^{17+}(nl_j) \tag{1}$$

that can be quantified in terms of populations $P(nl_j)$ (the fraction of outgoing ions in a given internal fine-structure

*marek.seliger@uni-graz.at

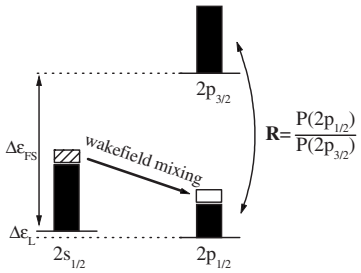

FIG. 1. Schematic diagram of the coherent mixing process in the $n=2$ manifold of Ar^{17+} due to the wake field during transport through carbon foils. The vertical axis indicates energy splitting and the height of the bars is proportional to the occupation probability. The patterned area corresponds to the overall amount of population shifted by wake-field mixing in transport through the thickest foil.

state nl_j) or capture cross sections. In this work we focus specifically on the ratio of the populations of the $2p_{1/2}$ and $2p_{3/2}$ states,

$$R = \frac{P(2p_{1/2})}{P(2p_{3/2})}. \tag{2}$$

Because nonrelativistic (NR) calculations for charge transfer include only spin independent interactions, the populations $P^{\mathrm{NR}}(nl_j)$ are determined by the populations of orbital angular momentum states, $P^{\mathrm{NR}}(nl)$, i.e., independent of the spin. Specifically, $P^{\mathrm{NR}}(nl)$ can be transformed into the fine-structure basis simply using statistical factors

$$P^{\mathrm{NR}}(nl_j) = \frac{1}{2}\frac{2j+1}{2l+1}P^{\mathrm{NR}}(nl). \tag{3}$$

For the $n=2$ level, Eq. (3) yields a nonrelativistic ratio

$$R^{\mathrm{NR}} = \frac{P^{\mathrm{NR}}(2p_{1/2})}{P^{\mathrm{NR}}(2p_{3/2})} = 0.5. \tag{4}$$

Equations (3) and (4) are a consequence of the disparate time scales for the atomic collision τ_{AC} and the characteristic fine-structure precession time $\tau_{\mathrm{FS}}, \tau_{\mathrm{AC}} \ll \tau_{\mathrm{FS}}$. Deviations from this value can be used to sensitively probe spin dependent and relativistic effects. Clearly, for ion-solid transmission with multiple collisions and wake-field mixing present (Fig. 1), the excited atomic states are subject to interactions on a much longer time for transmission (T), $\tau_{\mathrm{T}}=d/v_{\mathrm{p}}$ (d: typical thickness of the foil) $\tau_{\mathrm{T}} \gtrsim 1$ fs. This time scale is, typically, larger than τ_{FS}. Therefore deviations from the value $R^{\mathrm{NR}}=0.5$ are to be expected in ion-solid collisions.

This ratio is experimentally accessible with the help of high-resolution x-ray spectroscopy of photons emitted in the relaxation cascade after the interaction (for details see [7,6]). To reach high precision in the measurement of Lyman intensities $I(np \rightarrow 1s)$, we employ high-transmission high-resolution Bragg-crystal spectrometers specifically designed for this type of experiment resolving the two fine-structure $2p_j$ components. Populations are deduced from emission intensities $I(np_j \rightarrow 1s)$. Because these intensities include contributions from radiative relaxation of higher excited states,

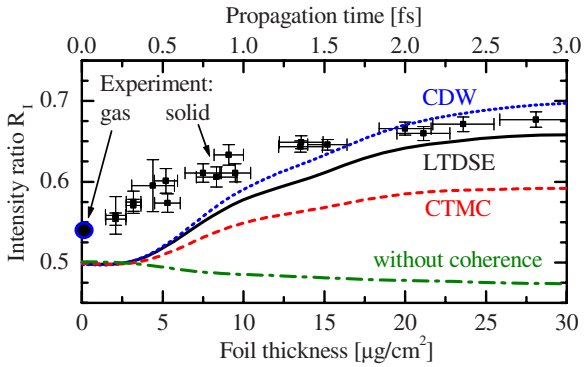

FIG. 2. (Color online) Lyman-α photon intensity ratio R_{I} between $2p_{1/2} \rightarrow 1s$ and $2p_{3/2} \rightarrow 1s$ following transport of Ar^{17+} ions (initially Ar^{18+}) through carbon foils as a function of foil thickness and the corresponding propagation time. Symbols: experiment with solid and gaseous (CH_4) targets; lines: calculations with different capture density matrices as source; dash-dotted line: calculation neglecting the wake field (equivalent to neglecting coherences).

the ratio of intensities are closely related, but not strictly equivalent, to Eq. (2). We focus here on the ratio

$$R_{\mathrm{I}} = \frac{I(2p_{1/2} \rightarrow 1s_{1/2})}{I(2p_{3/2} \rightarrow 1s_{1/2})}, \tag{5}$$

where the spectrometer efficiency does not vary significantly over this small energy interval such that systematic uncertainties cancel out. The remaining errors are expected to originate only from statistical uncertainties and Bremsstrahlung background. Experiments have been performed on the LISE (Ligne d'Ions Super Epluchés) facility at GANIL (Grand Accélérateur National d'Ions Lourds-Caen, France). Our simulations of R_{I} include cascade contributions which replenish the population of the $p_{3/2}$ and $p_{1/2}$ states.

III. RESULTS AND DISCUSSION

The ratio R_{I} for Ar^{17+} formed by charge transfer into bare Ar^{18+} ions transmitted through carbon foils at varying thicknesses at a speed of $v_p=23$ a.u. (Fig. 2) clearly displays spin-dependent relativistic effects. The measured ratio of intensities can be as large as $R_{\mathrm{I}}=0.66$ for the largest foil thicknesses. In the single collision limit of very thin foils the ratio decreases to a value close to ~0.5 but is systematically about ~10% larger than expected. In order to identify the true single collision limit, we have also performed experiments using fully stripped Ar^{18+} ions that are directed onto a gaseous carbon target (CH_4). Due to the long mean free path (MFP) for capture the projectile interacts only once with the dilute gas. Measurements with N_2 gas targets show similar results (i.e., the nuclear charge $Z_{\mathrm{T}}=7$ is very similar to that of C, $Z_{\mathrm{T}}=6$). Experimentally, whatever the gas (CH_4 or N_2) is, we find a value of $R_{\mathrm{I}}=0.54 \pm 0.011$.

Figure 2 displays the result of several simulations for the interaction with carbon foils using the method described in [6]. The simulations predict the outgoing distribution of excited states in solids by means of a partially coherent multistep process. First, charge transfer in a close collision be-

tween the projectile and a target atom takes place [Eq. (1)]. Subsequently, the hydrogenic ion is transported through the solid whereupon mixing among the excited states occurs as a result of collisions with both multiple target electrons and ionic core and the wake field induced by the moving ion. The interaction with the radiation field, specifically radiative transitions between projectile states which lead to population transfer during the transport, is included in the transport simulation for this system. Most of the Lyman-α radiative decay measured occurs, however, in vacuum, i.e., after the ion has left the foil. While for transport and radiative decay relativistic fine-structure corrections are included, our most reliable calculation for the primary electron capture step is the numerical solution of the nonrelativistic time-dependent Schrödinger equation on a lattice (LTDSE) [10] for the single-electron $Ar^{18+}+C(1s)$ collision system. In order to test the sensitivity of the excited state distribution formed by electron capture, we also present results using other well established nonrelativistic calculations: the classical trajectory Monte Carlo (CTMC) method [11–13] and the continuum-distorted wave (CDW) approximation [14,15].

Since all simulations shown in Fig. 2 treat the electron nonrelativistically (on the time scale τ_{AC}), they tend to the same ratio $R_I \sim 0.5$ in the single collision limit of very thin foils (i.e., as expected for the nonrelativistic ratio of the populations [Eq. (4)]. Conversely, all simulations exhibit a clear spin dependent effect for increasing foil thickness that is included in our open quantum system approach for transport through the solid by relativistic fine-structure effects [6]. We follow the time evolution of the one-electron density matrix, σ, of the electron attached to the projectile. Its diagonal elements in a fine-structure basis, $P_i=\sigma_{i,i}$, give the population of fine-structure states nl_j. Relativistic corrections included are the fine-structure and Lamb splitting of the energy levels and the radiative decay. The departure from $R_I \sim 0.5$ seen in our simulations for increasing foil thickness is a direct consequence of the interplay between the wake field generated in the solid by the moving ion and the relativistic splitting of the energy levels of the ion, both of which are relevant on the time scale of the typical passage time through the foil (i.e., $\tau_{FS} < \tau_W < \tau_T$).

The influence of the wake field is closely linked to the fact that the evolution of the excited-state population proceeds in a partially coherent fashion. The capture as a "source" generates a coherent substate population characterized by nonvanishing off-diagonal density matrix elements $\sigma_{i,j}$ which evolve under the influence of decohering multiple collisions, yet transiently survive. The coherent superposition of different eigenstate wave functions with a fixed phase relation leads for nondegenerate states to quantum beats between these states [16,17] that can be detected with the help of an external electric field [18,19]. Figure 3 shows the evolution of the absolute magnitude of coherences $|\sigma_{i,j}|$ in the $n=2$ manifold. The dominant feeding process of coherences for thin foils is the direct electron capture from $C(1s)$ (for thicker foils than those displayed also electron capture into $Ar^{17+}(1s)$ followed by excitation to $n=2$ plays an important role).

Initially, coherences grow in magnitude for increasing thickness as an increasing fraction of ions capture an elec-

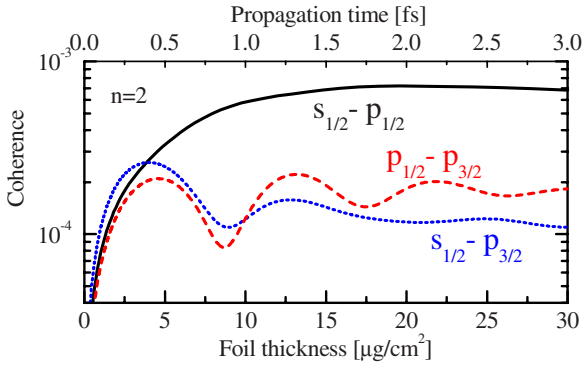

FIG. 3. (Color online) Absolute magnitude $|\sigma_{i,j}|$ of off-diagonal elements of the density matrix in $n=2$ as a function of foil thickness ($v_p=23$ a.u., initial charge state: Ar^{18+}).

tron. The growth is eventually disrupted as decoherence (dephasing and damping) sets in. Damping is due to stochastic collisions and radiative decay processes. The damping length for the present system is $L_D \approx 2000$ a.u. for $n=2$ corresponding to a damping time $\tau_D \approx 2$ fs. In turn, one major contribution to dephasing is the spread in time of the initial production of the excited state. In other words, the density matrix represents an ensemble average of excited states produced by electron capture at different times as the ion penetrates the solid. Coherences $\sigma_{i,j}$ that are produced at different times (propagation distances) separated by τ ($D=v_p\tau$) dephase as $\tau|E_i-E_j| \cong 2\pi$. For off-diagonal elements involving the fine-structure splitting (e.g., $\sigma_{2s_{1/2},2p_{3/2}}$) the dephasing time is $\tau_{FS} \approx 0.9$ fs corresponding to a propagation length of $D_{FS} \approx 860$ a.u. For elements separated by the Lamb shift (e.g., $\sigma_{2s_{1/2},2p_{1/2}}$), $\tau_L \approx 26$ fs with $D_L \approx 25\,000$ a.u.. Since τ_{FS} is smaller than τ_D, the $2s_{1/2}-2p_{3/2}$ and $2p_{1/2}-2p_{3/2}$ coherences resemble the shape of $|\sin(\pi d/D_{FS})|$ where the minima are located at propagation distances d that are integer multiples of D_{FS}. In turn, the $2s_{1/2}-2p_{1/2}$ coherence (split by Lamb shift) is governed by damping (multiple collisions and radiative decay) since $\tau_L \gg \tau_D$ (or $D_L \gg L_D$). Nevertheless, this coherence is not entirely damped out because of the continuous feeding by electron capture [and collisional excitation from $Ar^{17+}(1s)$]. The excited-state coherences get replenished continuously and a transient dynamical equilibrium is reached. The value of the coherence for thick foils is determined by the interplay of decoherence and buildup of coherence which compensate each other in this limit.

The wake field W which acts like an effective electric field leads to a Stark mixing of nearly degenerate states of opposite parity. Therefore it couples to first order in W off-diagonal elements σ_{s,p_j} ($j=1/2,3/2$) to diagonal elements σ_{p_j,p_j}. The strength of the coupling is of the order of $W\langle z\rangle_{i,j}/|E_i-E_j|$ with the dipole matrix element $\langle z\rangle_{i,j}$ between the states i and j [20]. Therefore fine-structure state populations are sensitive to the wake field W and to the relativistic splittings $|E_i-E_j|$. At the same time, they also can provide information on the coherence and decoherence during excitation and transport. This interplay is illustrated in Fig. 2 where we also show a simulation where we omit the wake field. From the above analysis it follows that this is equivalent to neglecting coherences (i.e., setting $\sigma_{i,j}=0$). In either

case, we find R_I to be nearly constant and, in fact, slightly decreasing. The latter is due to cascade contributions.

In the presence of the wake field R_I increases with increasing propagation distance since the transfer is directed from the $2s_{1/2}$ to the $2p_{1/2}$ state. The direction of this transfer is directly related to the signs of both the wake field and initial coherence between these two states immediately after an electron capture event [20]. Calculations of charge transfer [6] show that this coherence is nearly purely imaginary and negative, $\sigma_{2s_{1/2},2p_{1/2}} \sim -i\sqrt{P_{2s_{1/2}} P_{2p_{1/2}}}$, which dictates the initial direction of the flow of probability after electron capture. Since the wake field Stark coupling $W|<2s_{1/2}|z|2p_{1/2}>| \approx 0.06$ a.u. (≈ 1.6 eV) is larger than the Lamb shift of $|E_{2s_{1/2}} - E_{2p_{1/2}}| = 0.0052$ a.u. (or 0.16 eV) but smaller than the fine-structure splitting $|E_{2p_{3/2}} - E_{2s_{1/2}}| = 0.17$ a.u. (or 4 eV), the $2p_{3/2}$ state becomes partially "decoupled" from the $2p_{1/2}$ and $2s_{1/2}$ states which, in turn, are strongly mixed. Calculations using the TDSE and CDW methods for electron capture approximately reproduce the behavior of the experimental data for increasing foil thickness. However, a clear discrepancy is evident in the single collision limit of very thin foils, i.e., on a shorter time scale τ_{AC}, where fine-structure effects can be clearly ruled out. This strongly hints at additional relativistic effects that are not accounted for in the simulations. Post-collisional Stark mixing in the primary ion-atom collision event (qualitatively similar to the wake-field mixing discussed above) is ineffective to cause any spin dependence [20] since $\tau_{AC}/\tau_{FS} \ll 1$. Therefore additional spin dependent effects should be present in the primary charge transfer process on the time scale τ_{AC}.

To estimate whether additional relativistic effects are present during binary collisions, we have employed the relativistic eikonal approximation (REA) [1–3]. Input data for the collision system considered here were provided to us by the authors of those articles [21]. The total capture cross sections from $C(1s)$ and $C(2s)$ to $Ar^{17+}(2p_{1/2})$ and $Ar^{17+}(2p_{3/2})$ are given by 1.562×10^{-22} cm^2 and 3.004×10^{-22} cm^2, respectively. Since the nonrelativistic part of the capture process (i.e., summed over spin degrees of freedom) is described less accurately we expect the absolute magnitude of these cross sections to be less accurate (they are, in fact, lower than those predicted by either the LTDSE or the CDW approximation which approximately agree with the experiment [6]). By considering only the ratio of fine-structure split states we hope to partly account for the relativistic effects of the dynamics described by the relativistic formulation of the eikonal theory and mask its deficiency in the nonrelativistic regime. This approach is motivated by the lack of a full relativistic calculation of the capture process on a lattice (like the accurate LTDSE for nonrelativistic capture) for this intermediate velocity regime. The REA predicts a ratio $R=0.52$, i.e., different from $R=0.5$, and thus gives a clear hint that additional relativistic corrections could be present. In order to analyze the consequences of such an increased ratio of populations, we have modified the capture density matrix σ^{LTDSE} such that the ratio R is enhanced to the value found by the REA, i.e., $R=0.52$ while preserving the trace, $\mathrm{Tr}_{n=2}[\sigma]$. Such a change is still insufficient to account for the data (Fig. 4). This is, in part, due to cascade contributions which tend to lower rather than to increase R_I. Accordingly, in order to adjust the ratio R in σ^{LTDSE} such that R_I resembles the value of $R_I=0.54$ in the single collision regime a shift to $R=0.56$ is necessary (Fig. 4). Remarkably, adjusting the initial R to this value in the limit $d \to 0$ leads to excellent agreement in the entire range of thicknesses (or distances of propagation) shown in Fig. 4. This provides a strong hint that relativistic effects of that order of magnitude are, indeed present in the density matrix for one-electron capture at moderately relativistic velocities. However, a microscopic justification for the magnitude of this effect is lacking and poses an open question for future theoretical studies of relativistic atomic collisions.

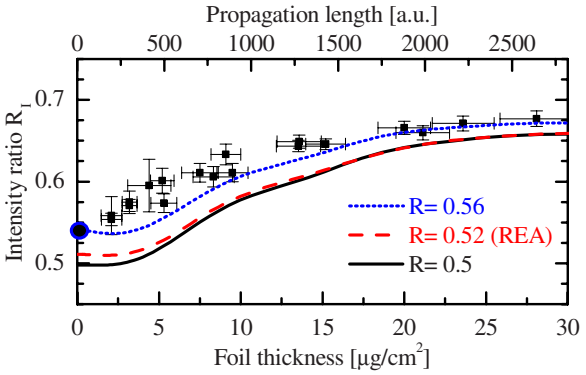

FIG. 4. (Color online) As in Fig. 2, but for modified initial density matrix using LTDSE but with adjusted ratio $\sigma_{2p_{1/2}}/\sigma_{2p_{3/2}}$ (see text); dotted line: optimized value for gas target $R=0.56$; dashed line: $R=0.52$ from REA.

IV. CONCLUSIONS

We have shown that the ratio of populations of the fine-structure states $2p_{3/2}$ and $2p_{1/2}$ is remarkably sensitive to relativistic corrections, to wake-field effects, and collisionally induced transient coherences. The ratio varies significantly as a function of the distance of propagation in transport of moderately relativistic highly charged ions through solids. Changes as a function of penetration length are well accounted for by our quantum transport simulation. Remarkably, in the limit of small propagation distances, e.g., in the single-collision limit a systematic discrepancy persists that suggests the presence of relativistic corrections in the primary atomic charge transfer process. Preliminary calculations employing the relativistic eikonal approximation provide hints in this direction but a definite quantitative description remains an open question.

ACKNOWLEDGMENTS

This work was supported by the FWF (Austria) special research project SFB016 "ADLIS," by the FWF projects P15025-N08 and P16871-NO8, and by EU projects HITRAP (HPRICT-2001-50036) and ITS-LEIF (HPRI-CT-2005-026015). This work was also supported by the U.S. DOE

Office of Fusion Energy Sciences, including a SciDAC grant administered through Auburn University, and from the Office of Basic Energy Sciences, to Oak Ridge National Laboratory which is managed by UT-Battelle, LLC under Contract No. DE-AC05-00OR22725. We would like to acknowledge helpful discussions with Jörg Eichler and Akira Ichihara. We address specific thanks to the staff of CIRIL and GANIL for providing us with outstanding technical assistance and exceptional high-quality beams. We are also grateful to Lamri Adoui, Amine Cassimi, Brigitte Ban d'Etat, Benoit Gervais, Celine Lauhlet, Medhi Tarisien, and Jean Marc Ramillon for their participation in the data acquisition.

[1] J. Eichler, Phys. Rev. A **32**, 112 (1985).
[2] J. Eichler, Phys. Rep. **193**, 165 (1990).
[3] A. Ichihara, T. Shirai, and J. Eichler, At. Data Nucl. Data Tables **55**, 63 (1993).
[4] J. Eichler and T. Stöhlker, Phys. Rep. **439**, 1 (2007).
[5] X. Ma, T. Stöhlker, F. Bosch, O. Brinzanescu, S. Fritzsche, C. Kozhuharov, T. Ludziejewski, P. H. Mokler, Z. Stachura, and A. Warczak, Phys. Rev. A **64**, 012704 (2001).
[6] M. Seliger, C. O. Reinhold, T. Minami, D. R. Schultz, M. S. Pindzola, S. Yoshida, J. Burgdörfer, E. Lamour, J. P. Rozet, and D. Vernhet, Phys. Rev. A **75**, 032714 (2007); M. Seliger, Ph.D. thesis, Vienna University of Technology, Vienna, 2005.
[7] E. Lamour, B. Gervais, J.-P. Rozet, and D. Vernhet, Phys. Rev. A **73**, 042715 (2006).
[8] M. Seliger, C. O. Reinhold, T. Minami, and J. Burgdörfer, Phys. Rev. A **71**, 062901 (2005).
[9] T. Minami, C. O. Reinhold, and J. Burgdörfer, Phys. Rev. A **67**, 022902 (2003).
[10] T. Minami, C. O. Reinhold, D. R. Schultz, and M. S. Pindzola, J. Phys. B **37**, 4025 (2004).
[11] R. Abrines and I. C. Percival, Proc. Phys. Soc. **88**, 861 (1966).
[12] R. E. Olson and A. Salop, Phys. Rev. A **16**, 531 (1977).
[13] C. O. Reinhold and C. A. Falcon, Phys. Rev. A **33**, 3859 (1986).
[14] I. M. Cheshire, Proc. Phys. Soc. London **84**, 89 (1964).
[15] J. Burgdörfer and L. J. Dubé, Phys. Rev. Lett. **52**, 2225 (1984); Phys. Rev. A **31**, 634 (1985).
[16] C. C. Havener, N. Rouze, W. B. Westerveld, and J. S. Risley, Phys. Rev. A **33**, 276 (1986).
[17] J.-P. Rozet, D. Vernhet, I. Bailly-Despiney, C. Fourment, and L. J. Dubé, J. Phys. B **32**, 4677 (1999).
[18] H. J. Andrä, Phys. Rev. Lett. **25**, 325 (1970).
[19] D. Schneider, W. Zeitz, R. Kowallik, G. Schiwietz, T. Schneider, N. Stolterfoht, and U. Willie, Phys. Rev. A **34**, 169 (1986).
[20] J. Burgdörfer, Phys. Rev. A **24**, 1756 (1981); J. Burgdörfer, Ph.D. thesis, Freie Universität, Berlin, 1981.
[21] J. Eichler and A. Ichihara (private communication).